

NASA Technical Memorandum 107123 _____
AIAA-96-0495

7539
P-11

3D Navier-Stokes Analysis of a Mach 2.68 Bifurcated Rectangular Mixed- Compression Inlet

M. Mizukami and J.D. Saunders
Lewis Research Center
Cleveland, Ohio

Prepared for the
34th Aerospace Sciences Meeting and Exhibit
sponsored by the American Institute of Aeronautics and Astronautics
Reno, Nevada, January 15-18, 1996



National Aeronautics and
Space Administration

(NASA-TM-107123) THE 3D
NAVIER-STOKES ANALYSIS OF A MACH
2.68 BIFURCATED RECTANGULAR
MIXED-COMPRESSION INLET (NASA.
Lewis Research Center) 11 p

N96-17819

Unclass

G3/07 0098295

3D NAVIER-STOKES ANALYSIS OF A MACH 2.68 BIFURCATED RECTANGULAR MIXED-COMPRESSION INLET

M. Mizukami and J. D. Saunders
NASA Lewis Research Center
Cleveland, Ohio 44135

Abstract

The supersonic diffuser of a Mach 2.68 bifurcated, rectangular, mixed-compression inlet was analyzed using a three-dimensional (3D) Navier-Stokes flow solver. A two-equation turbulence model, and a porous bleed model based on unchoked bleed hole discharge coefficients were used. Comparisons were made with experimental data, inviscid theory, and two-dimensional Navier-Stokes analyses. The main objective was to gain insight into the inlet fluid dynamics. Examination of the computational results along with the experimental data suggest that the cowl shock-sidewall boundary layer interaction near the leading edge caused a substantial separation in the wind tunnel inlet model. As a result, the inlet performance may have been compromised by increased spillage and higher bleed mass flow requirements. The internal flow contained substantial waves that were not in the original inviscid design. 3D effects were fairly minor for this inlet at on-design conditions. Navier-Stokes analysis appears to be an useful tool for gaining insight into the inlet fluid dynamics. It provides a higher fidelity simulation of the flowfield than the original inviscid design, by taking into account boundary layers, porous bleed, and their interactions with shock waves.

Nomenclature

x	axial coordinate, from ramp tip
y	vertical coordinate, from centerline
h_c	cowl half-height
p	static pressure
p_T	total pressure

Subscripts

o	freestream
-----	------------

Introduction

On supersonic cruise aircraft at Mach numbers above 2.0 to 2.2, mixed-compression inlets are used to achieve high total pressure recovery and low cowl drag. However, mixed compression inlets are susceptible to unstarts, where the normal shock wave is expelled forward out of the inlet, total pressure recovery is drastically reduced, and severe forces may result on the aircraft. The angle of attack or Mach number reduction the inlet can tolerate before unstating is a measure of the inlet's operability limit. Boundary layer bleed is used to condition the shock boundary layer interactions, and to help stabilize the normal shock and prevent unstarts. Due to the complexity of interactions, bleed patterns are typically laid out using empirical guidelines. Overall, the design of a supersonic mixed compression inlet is a balance between the conflicting requirements of internal performance, external drag, operability and weight.^{1,2,3}

Supersonic diffusers for mixed compression inlets are generally designed using inviscid analyses. The method of characteristics is typically used, because of its exact inviscid results and fast turnaround time. The actual flowfield differs from the inviscid analysis, due to additional viscous effects and interactions. Therefore, a number of analysis techniques accounting for these effects have been developed, to more accurately predict the performance and flowfield.

In a zonal approach, the flowfield is partitioned into distinct areas depending on the dominant physics, and each area is analyzed using a separate technique. Typically, the inviscid core is computed using the method of characteristics, near wall areas are solved with a boundary layer code, bleed regions are modeled by manipulating the boundary layer profiles, and oblique shock-boundary layer interactions are solved using control volume analysis. The zonal approach is useful for rapidly evaluating a large number of configurations, and for determining boundary layer properties in order to place bleed regions. However, more complex flows, such as corner flows, subsonic regions, separations and vortices, are difficult to model properly. Therefore, 3D flows, normal shocks, and operability limits are not accurately simulated.

In reduced or 'parabolized' Navier Stokes (PNS) analysis, the streamwise diffusion term is neglected.

For supersonic flow, this allows the solution to be marched downstream in space, computing only one axial plane at a time. As a result, PNS is computationally efficient, and it is well suited for modeling supersonic diffusers, including 3D effects. However, PNS may not properly simulate inherently elliptical flow features such as large subsonic regions and separated flows. Therefore, it may not be suitable for determining operability limits.

Although full Navier-Stokes analysis is computationally expensive, its main advantage is generality. Complex flows and interactions such as corner flows, glancing shock-boundary layer interactions, normal shocks and separated flows can be modeled, at least in principle. Therefore, within the limits of available computational resources, almost all aspects of the inlet flow could be simulated, including operability limits, terminal shocks, and subsonic diffuser flow. General purpose Navier-Stokes solvers can be used with only minor modifications, minimizing the code development and validation effort. However, many issues remain to be considered, such as truncation error, accuracy of turbulence models, and grid sensitivity⁴.

A number of Navier-Stokes solutions of mixed compression inlets have been reported in the literature. Of particular interest here are 3D Navier-Stokes analyses of rectangular supersonic inlets. Rectangular inlets are complicated by sidewall and corner effects, that are not present in axisymmetric inlets or in the original inviscid design. Shigematsu et al⁵ reported a two-dimensional (2D) solution of a rectangular inlet in supercritical operation, and a 3D solution of the supersonic diffuser, both using the Baldwin-Lomax algebraic turbulence model. They obtained qualitative agreement with data in the limited comparisons, and stated that the turbulence model would have to be investigated to improve the results. Reddy and Weir⁶ showed substantial 3D effects in a Mach 5 rectangular inlet, and obtained good qualitative agreement with data, using an algebraic turbulence model and a simple uniform mass flux bleed boundary condition. It was again suggested that a better turbulence model would improve simulation of the corner flows. Fujimoto and Niwa⁷ reported a 3D calculation of a rectangular inlet including the terminal shock. Good agreement was shown with data, and a vortex was seen along the cowl shock-sidewall interaction. Freskos and Penanhoat⁸ produced 2D and 3D solutions of a Mach 1.865 rectangular inlet including the terminal shock, but did not report any comparisons with data.

A medium scale model of a Mach 2.68 bifurcated rectangular mixed compression inlet with 30% internal area contraction was tested in the NASA Lewis 10x10

foot cross section supersonic wind tunnel (Figs. 1, 2).⁹ Note that the sidewall leading edge extends slightly forwards of the cowl leading edge. The freestream Reynolds number at Mach 2.68 was 2.5×10^6 per foot, and the cowl half-height (h_c) was 10.67 inches. Figure 3 shows the theoretical shock structure, designed using the method of characteristics. The initial ramp shock is followed by an isentropic compression fan, both focused on the cowl lip. The initial cowl shock is also followed by an isentropic compression fan; the cowl shock is canceled at the ramp shoulder, and the compression fan is canceled on the curved ramp surface. In the test program, parametrics were performed on the freestream Mach number, angle of attack, bleed patterns, subsonic diffuser vortex generator patterns, and ramp positions. Three configurations were selected for detailed study, two of which had the ability to self-start following an unstart without active controls. One of the self starting configurations gave 89 percent total pressure recovery and 16 percent distortion at the compressor face station, with a bleed massflow of 6.9 percent of capture, in critical operation. The spillage of about 4.6 percent of capture was much higher than expected.

In previous 2D Navier-Stokes analysis of this inlet¹⁰, extensive parametrics were performed on turbulence models, computational grids and bleed models. The solutions were found to be fairly insensitive to these parametrics. An algebraic, one-equation and two-equation turbulence models were examined. The two-equation k- ϵ model of Chien¹¹ was recommended, because it is applicable to a wider range of flows than the simpler models, while it is more appropriate to use in an engineering environment than the more elaborate techniques, such as Reynolds stress modeling or large eddy simulation. Four models for porous bleed were evaluated. The 'unchoked hole' model was recommended, because it is the most realistic simulation, and because it provides a prediction of bleed mass flow rates. Local wall mass flux was determined based on discharge coefficients of unchoked bleed holes, bleed region porosity, local flow conditions, and plenum back pressure.

In the present study, the supersonic diffuser of this Mach 2.68 bifurcated, rectangular, mixed-compression inlet was analyzed using a 3D Navier-Stokes flow solver. A two equation turbulence model, and a porous bleed model based on unchoked bleed hole discharge coefficients were used. Comparisons were made with experimental data, inviscid theory, and 2D Navier-Stokes analysis. The main objective was to gain insight into the inlet fluid dynamics.

Numerical Methods

The flow solver used in the present study is NPARC, a Navier-Stokes solver for compressible flows.^{12,13} The governing equations are the time dependent Reynolds averaged Navier-Stokes equations with a perfect gas relationship and Fourier's heat conduction law. These equations are discretized in conservation law form with respect to general curvilinear coordinates and solved with the Beam and Warming approximate factorization algorithm. Although the time dependent formulation of the governing equations is used, not all portions of the present version of the code are time-accurate, and it is intended for steady state simulations. Viscous terms were included in all three dimensions, and default artificial viscosity settings were used.

As recommended in the previous 2D parametric study, the Chien k- ϵ turbulence model and the unchoked hole porous bleed model were used. An algorithm was implemented for irregularly shaped bleed regions that do not follow the grid lines, such as the forward sidewall bleed.

The unchoked hole bleed model determines local wall mass flux based on discharge coefficients of unchoked bleed holes, bleed region porosity, local flow conditions, and plenum back pressure. The discharge coefficient curves were based on experimental results of Syberg and Hickcox¹⁴. The tangential velocity at the wall was set to zero, and the static pressure and temperature gradients normal to the wall were prescribed to be zero. Strictly speaking, these boundary conditions are not physically correct, but they are consistent with the treatment of solid no-slip walls in the flow solver. No attempt was made to model the roughness effect of the porous bleed surface.

A cross section of the computational grid is shown in Figure 4. The grid consists of approximately 714,000 grid points in 4 blocks (Table 2). All internal wall regions were packed to a typical y^+ value of 2, as calculated from the solution. The external grid was fairly coarse. In order to resolve the shock waves more crisply, the grid was adapted as much as possible to the initial ramp shock and the cowl shock by slanting the cross-stream grid lines. The cowl lip was as sharp as the grid packing at the wall would allow, about 0.0001 inch thick. Taking advantage of the two planes of symmetry, only one quadrant of the inlet was analyzed.

All internal walls were assumed to be turbulent, and all external walls were treated as slip surfaces. Flow conditions were fixed at the inflow plane and on all external planes parallel to the freestream flow. The boundary condition at the exit plane was extrapolated.

Two configurations were investigated. The 'SS1'

configuration has higher bleed mass flow rates, and was experimentally shown to be self-starting. The 'NSS' configuration has less bleed, but was not self-starting.

The flow solver was run on a Cray Y-MP supercomputer. For each configuration, approximately 10000 iterations were run, with a time step CFL number of 0.3. The L2 residual norm bottomed out after a reduction of about 5 orders of magnitude. No appreciable change was observed in the solution over the last 1000 iterations.

Results

Results of the present 3D analysis are compared with 2D analysis using the same cross-sectional grid, previous 2D analysis in reference 10 using the same numerical methods and a finer grid, and experimental data of Wasserbauer et al⁹.

Mass flow rates and recoveries are shown in Table 1. Note that in the 2D analyses, corner and sidewall bleeds were neglected, and therefore the total amount of bleed was lessened. Bleed mass flow rates were predicted fairly well, with the notable exception of the forward sidewall, which was substantially underpredicted. Spillage was significantly underpredicted, although 3D indicates slightly more spillage than 2D. Mass flux averaged throat total pressure recoveries are comparable for 3D and 2D results, indicating that the sidewall boundary layer losses are negligible in the mass averaged sense.

Bleed patterns and rake locations for the SS1 configuration are shown in Figure 5a. In the centerline surface pressures (Fig. 5b), computational results and experimental data both show the cowl shock impinging on the ramp slightly in front of the shoulder. Both 3D and 2D results failed to predict the high pressure region on the cowl surface near $x/h_c = 3.1$, but 3D results predicted the lower pressures around $x/h_c = 3.3 \sim 3.5$. The boundary layer profile at the sidewall rake (Fig. 5c) was not well predicted. For the boundary layer rake just aft of the ramp shoulder (Fig. 5d) comparisons between computational results and data are inconclusive, because the accuracy of the experimentally derived total pressures may be somewhat questionable. At this rake location, the analysis shows the flow to be highly nonuniform due to reflected waves. Therefore, it is probably not very accurate to use the single static pressure tap measurement at the base of the rake to convert the rake pitot pressures to total pressures.

NSS configuration bleed patterns, rake locations, ramp and cowl pressures, and boundary layer profiles are shown in Figure 6. For this configuration, the surface pressures were qualitatively well predicted. In the

boundary layer profiles, the local overshoot above a pressure ratio of 1 is believed to be an artifact of the grid resolution. It is difficult to properly resolve this region with rapid gradient changes near the top of the boundary layer, especially in a 3D problem.

Visualization of the numerical results for the SS1 bleed configuration are shown in figure 7. As seen in the centerline Mach contours (Fig. 7a), the flow was appreciably different from the original inviscid design shown in Fig. 3. Sidewall, ramp, and cowl pressure contours (Figs. 7b, 7c and 7d) show that bleed regions generated substantial waves, a complex interaction existed between cowl shock and the sidewall near the leading edge, and the ramp isentropic compression was steepened near the sidewall. Sidewall surface streamlines (Fig. 7e), or simulated 'oil flows', reveal several interesting features: the ramp isentropic compression caused a secondary flow toward the cowl, a small separation existed due to the cowl shock - sidewall boundary layer interaction near the leading edge, and the secondary flow caused the low energy fluid to collect near the middle of the sidewall. As seen in the detail view of the streamlines near the sidewall surface (Fig. 7f), there was indeed a separation vortex due to the cowl shock - sidewall boundary layer interaction near the leading edge.

Discussion

Examination of the computational results along with the experimental data suggest that the cowl shock-sidewall boundary layer interaction near the leading edge caused a substantial separation in the wind tunnel model. As a result, the inlet performance may have been compromised by increased spillage and higher bleed mass flow requirements. This separation was not evident from the data alone. The analysis appears to underpredict the extent of separation, as suggested by several discrepancies with experimental data, and past experience with this turbulence model. The spillage mass flow was underpredicted (Table 1). A large separated region near the cowl-sidewall corner leading edge may detach the cowl shock and even force some reverse flow out the front of the inlet, increasing the spillage mass flow. The forward sidewall bleed mass flow rate was significantly underpredicted (Table 1) for both bleed configurations, indicating that the pressure over at least part of the bleed region should have been higher, as might be caused by a large separated region. For the SS1 configuration, the experimentally observed high pressure region at the cowl centerline near $x/h_c = 3.1$ was not predicted (Fig. 5b); however, a large separated region would cause a shock wave to propagate

diagonally downstream toward the centerline, and appear as a high pressure region. Furthermore, waves arising from the two sidewalls would constructively interfere at the centerline, producing an even higher pressure. The sidewall boundary layer profile (Fig. 5c) was poorly predicted, indicating that the sidewall secondary flows such as the separated flow were not accurately simulated. Past studies have shown that the Chien $k-\epsilon$ turbulence model tends to underpredict separation due to adverse pressure gradients and shock interactions^{15,16}. A turbulence model that more accurately predicts separations should improve the accuracy of results.

Computational results and wind tunnel data both show substantial waves in the internal flow that were not in the original inviscid design, as seen in the surface static pressures (Figs. 5b, 6b) and contour plots (Figs. 7a-d). The near sonic internal flow was highly sensitive to even small perturbations in the near wall flow. Bleed regions were seen to generate waves due to streamline turning. At the start of the bleed region, the streamlines turn toward the wall, thus producing an expansion wave. Over the bleed region, the streamlines angle into the wall. At the end of the bleed region, the streamlines turn sharply away from the wall as the boundary layer thickens rapidly at the start of the solid wall, producing a compression wave. Boundary layer displacement effects caused the cowl shock to steepen, impinge on the ramp forward of the shoulder, and reflect off instead of being canceled.

3D effects were fairly minor for this inlet at on-design conditions. Although 3D results were quite similar to 2D results, some evidence of 3D flows were observed, such as waves generated by sidewall bleeds and flow migration on the sidewall. Flow separation due to the cowl shock-sidewall boundary layer interaction, which was underpredicted, may be responsible for additional 3D effects. As the operability limits are approached, 3D effects will become more prominent, as shock-boundary layer interactions become more severe, bleed mass flow rates increase and the flow approaches sonic conditions. Also, for higher Mach number inlets, viscous effects and bleed mass flow rates are greater, causing more significant 3D effects.

Overall, Navier-Stokes analysis appears to be a useful tool for gaining insight into the inlet fluid dynamics. Although the analysis does not necessarily match the data in all instances, it provides a higher fidelity simulation of the flowfield than the original inviscid design, by accounting for boundary layers, porous bleed, and their interactions with shock waves. Most of the discrepancies with data were traceable to particular sources. Therefore, when interpreting the results, it is important to be aware of the strengths and weaknesses of the analysis method.

Conclusions

The supersonic diffuser of a Mach 2.68 bifurcated, rectangular, mixed-compression inlet was analyzed using a three-dimensional (3D) Navier-Stokes flow solver. A two-equation turbulence model, and a porous bleed model based on unchoked bleed hole discharge coefficients were used. Comparisons were made with experimental data, inviscid theory, and two-dimensional (2D) Navier-Stokes analyses. The major conclusions were as follows:

Examination of the computational results along with the experimental data suggest that the cowl shock-sidewall boundary layer interaction near the leading edge caused a substantial separation in the wind tunnel model. As a result, the inlet performance may have been compromised by increased spillage and higher bleed mass flow requirements. This separation was not evident from the data alone. The analysis appears to underpredict the extent of separation, as suggested by several discrepancies with experimental data, and past experience with this turbulence model.

Computational results and wind tunnel data both show substantial waves in the internal flow that were not in the original inviscid design. These waves were generated by interactions of boundary layers, bleed and shock waves.

3D effects were fairly minor for this inlet at on-design conditions. 3D results were quite similar to 2D results, but some evidence of 3D flows were observed. In certain other circumstances, 3D effects may be more prominent.

Navier-Stokes analysis appears to be a useful tool for gaining insight into the inlet fluid dynamics. Although the analysis does not necessarily match the data in all instances, it provides a higher fidelity simulation of the flowfield than the original inviscid design, by accounting for boundary layers, porous bleed, and their interactions with shock waves.

References

- ¹Seddon, J. and Goldsmith, E. L., *Intake Aerodynamics*, AIAA Education Series, AIAA, New York, 1985.
- ²Goldsmith, E. L. and Seddon, J., ed., *Practical Intake Aerodynamic Design*, AIAA Education Series, AIAA, New York, 1993.
- ³Bowditch, D. N., "Some Design Considerations for Supersonic Cruise Mixed Compression Inlets." NASA TM X-71460, 1973.
- ⁴Paynter, G. C. and Tjonneland, E., "Accuracy

Issues in the Prediction of Supersonic Inlet Flows," ASME 92-GT-400, 1992.

⁵Shigematsu, J., Yamamoto, K., Shiraishi, K. and Tanaka, A., "A Numerical Investigation of Supersonic Inlet Using Implicit TVD Scheme," AIAA-90-2135, 1990.

⁶Reddy, D. R. and Weir, L. J., "Three-Dimensional Viscous Analysis of a Mach 5 Inlet and Comparison with Experimental Data," *J. Propulsion and Power*, Vol. 8, No. 2, 1992, pp. 432-440.

⁷Fujimoto, A. and Niwa, N., "Experimental and Numerical Investigation of Mach 2.5 Supersonic Mixed Compression Inlet," AIAA 93-0289, 1993.

⁸Freskos, G. and Penanhoat, O., "Numerical Simulation of the Flow Field Around Supersonic Air-Intakes," ASME 92-GT-206, 1992.

⁹Wasserbauer, J. F., Meleason, E. T. and Burstadt, P. L., "Experimental Investigation of The Performance of a Mach 2.7 Two Dimensional Bifurcated Duct Inlet with 30 Percent Internal Contraction," NASA TM to be released, 1995.

¹⁰Mizukami, M. and Saunders, J. D., "Parametrics on 2D Navier-Stokes Analysis of a Mach 2.68 Rectangular Bifurcated Mixed Compression Inlet," AIAA 95-2755, 1995.

¹¹Chien, K.-Y., "Predictions of Channel and Boundary-Layer Flows with a Low Reynolds Number Turbulence Model," *AIAA J.*, Vol. 10, No. 1, 1982, pp. 33-38.

¹²Cooper, G. K. and Sirbaugh, J. R., "PARC Code: Theory and Usage," AEDC-TR-89-15, 1989.

¹³A *User's Guide to NPARC, Version 2.0*, NPARC Alliance, 1994.

¹⁴Syberg, J. and Hickcox, T. E., "Design of a Bleed System for a Mach 3.5 Inlet," NASA CR-2187, 1972.

¹⁵Rodi, W. and Scheuerer, G., "Scrutinizing the k- ϵ Turbulence Model Under Adverse Pressure Gradient Conditions," *Trans. ASME*, Vol. 108, June 1986, pp. 174-179.

¹⁶De Henau, V., Raithby, G. D. and Thompson, B. E., "Prediction of Flows with Strong Curvature and Pressure Gradient Using the k- ϵ Turbulence Model," *Trans. ASME*, Vol. 112, March 1990, pp. 40-47.

Table 1 Summary of results

configuration	SS1				NSS			
	3D CFD	2D CFD	ref. 10 2D CFD	data	3D CFD	2D CFD	ref. 10 2D CFD	data
bleed mass flows (% capture)								
forward sidewall	1.17	n/a	n/a	2.06	0.72	n/a	n/a	1.52
ramp shoulder	1.53	1.62	1.55	1.40	1.47	1.52	1.43	1.40
mid diffuser	1.26	1.07	1.04	1.26	0.69	0.47	0.48	1.04
throat	2.23	2.10	2.11	2.70	2.15	1.28	1.35	2.20
TOTAL	6.19	4.79	4.72	7.42	5.03	3.27	3.27	6.16
spillage (% capture)								
spillage (% capture)	2.60	1.97	1.97	4.60	2.60	1.97	1.97	4.60
throat mass averaged total pressure recovery								
throat mass averaged total pressure recovery	0.955	0.956	0.954	n/a	0.948	0.951	0.948	n/a

Table 2 Computational grid

block	region	grid points
1	internal	252,000
2	internal	252,000
3	external	84,000
4	external	126,000
total		714,000

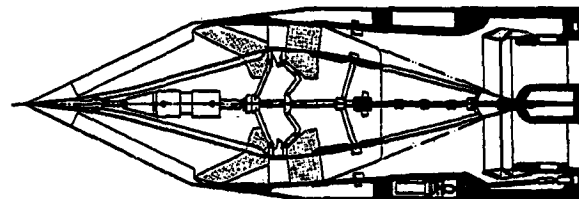


Fig. 2 Inlet model, centerline cross section.

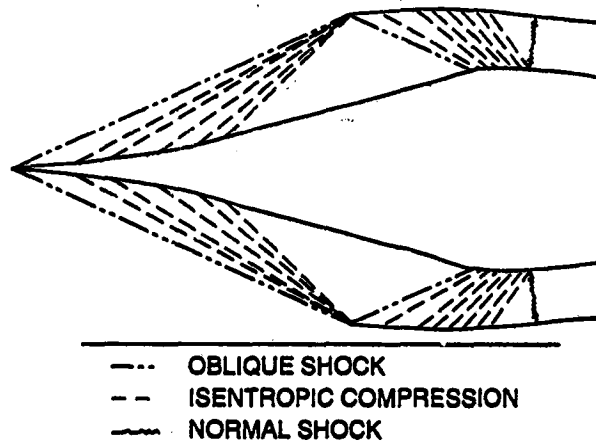


Fig. 3. Theoretical shock structure, on-design critical



Fig. 1 Inlet model in NASA Lewis 10x10 foot cross section supersonic wind tunnel.

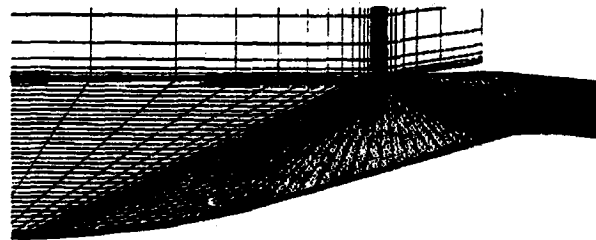



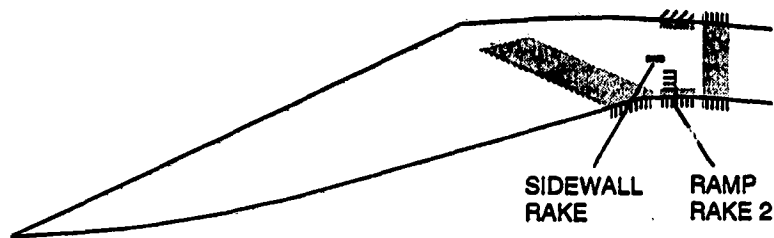
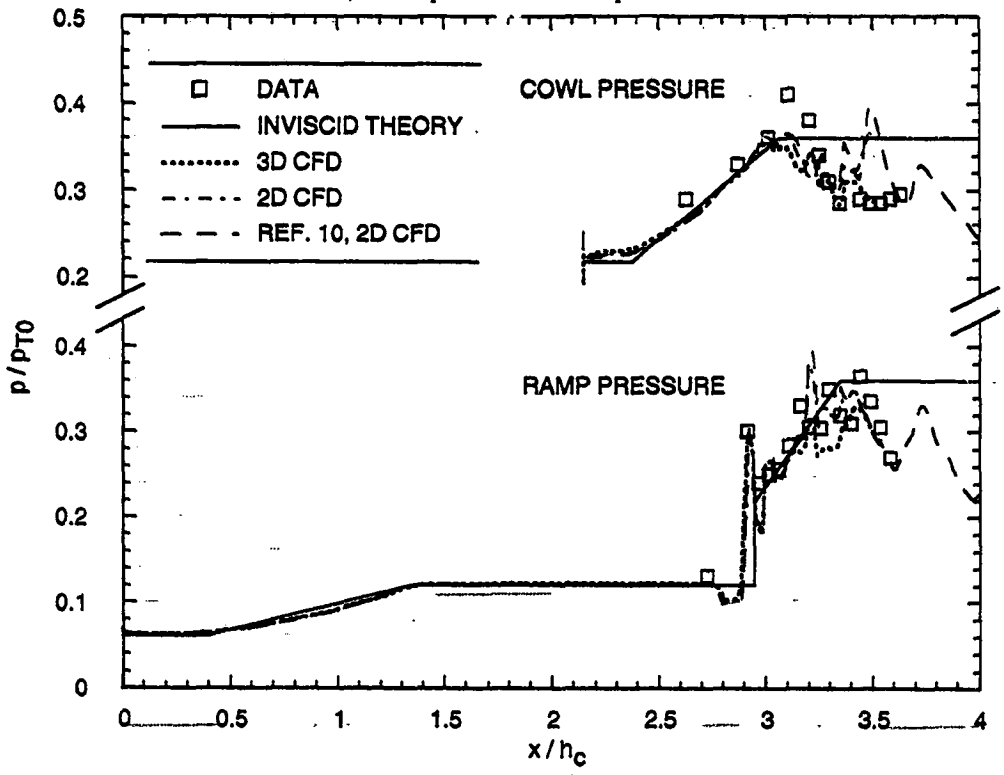


Fig. 4 Computational grid, centerline cross-section

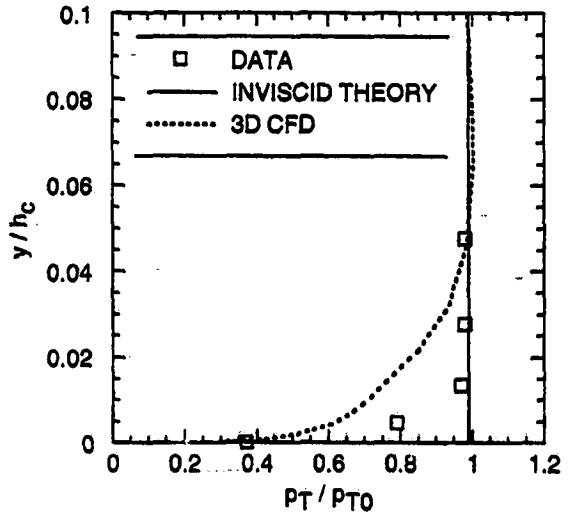
BLEED REGIONS	
	SIDEWALL
	RAMP AND COWL
	RAMP AND COWL CORNER



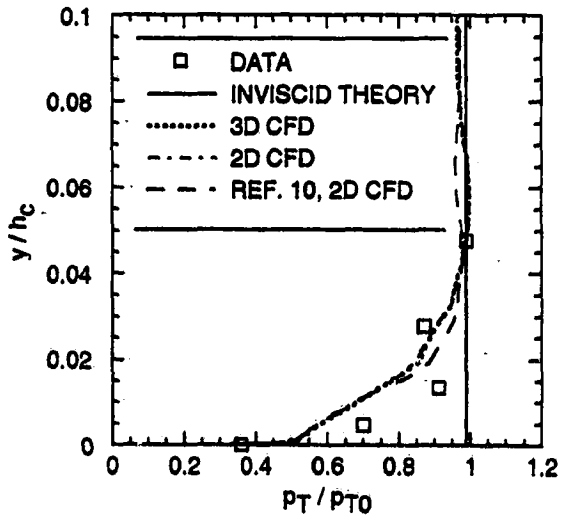
a) Bleed pattern and rake positions



b) Cowl and ramp centerline static pressures.

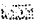




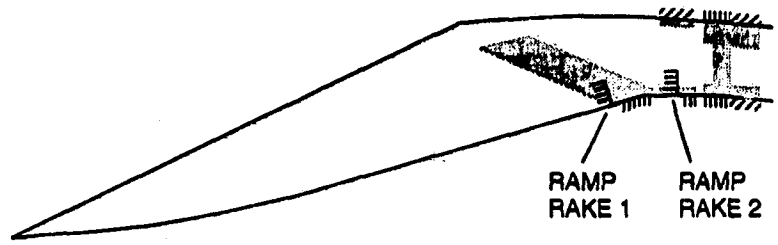
c) Sidewall rake



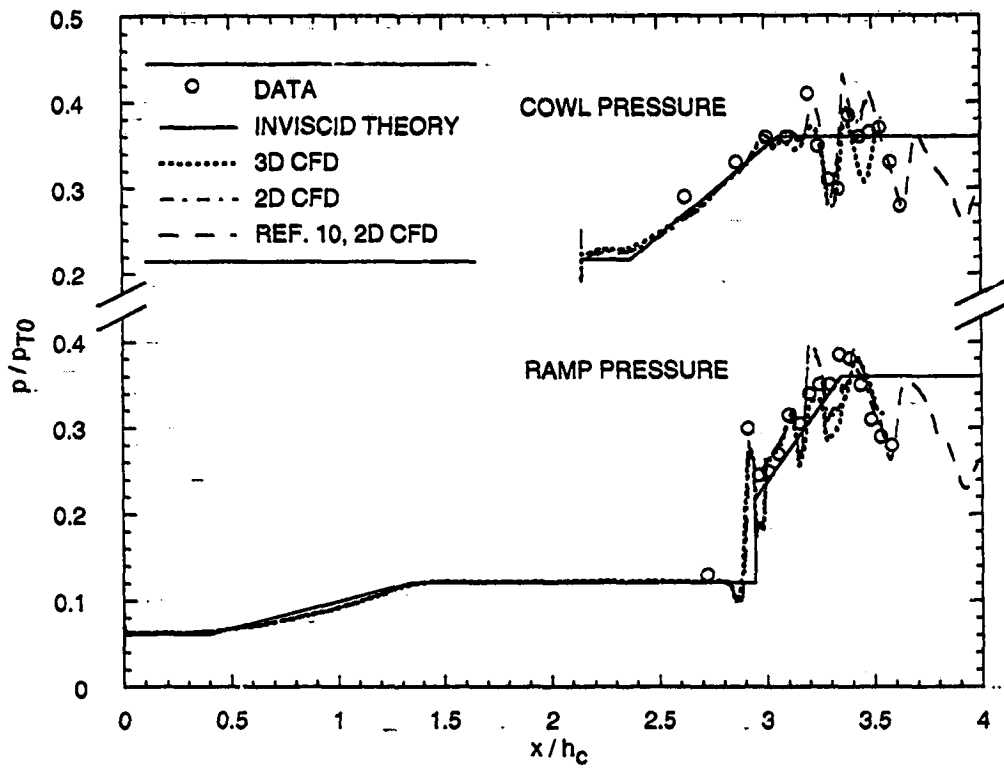
d) Ramp rake 2

Fig. 5 SS1 configuration results.

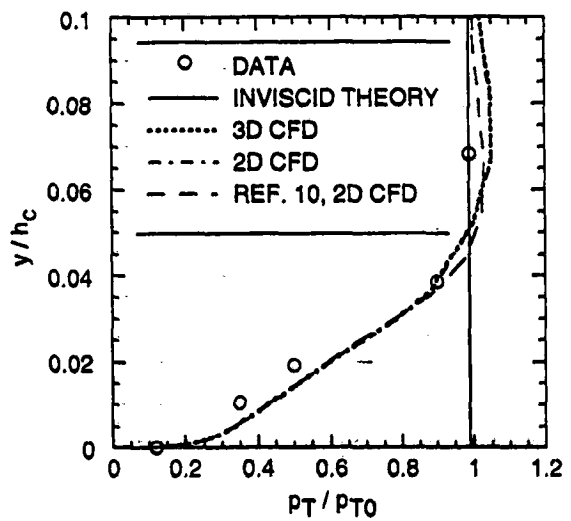
BLEED REGIONS	
	SIDEWALL
	RAMP AND COWL
	RAMP AND COWL CORNER



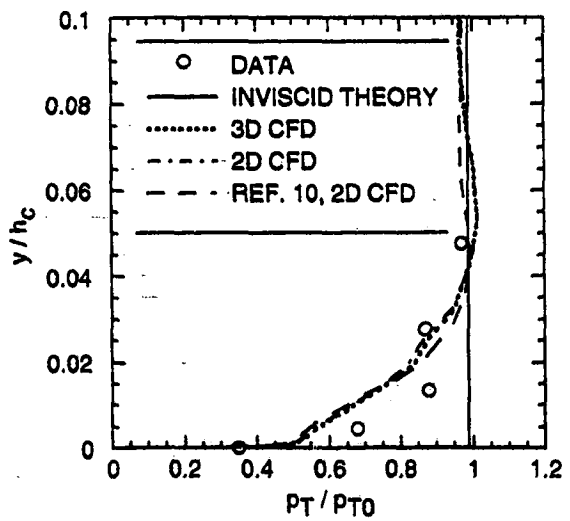
a) Bleed patterns and rake positions



b) Cowl and ramp centerline static pressures

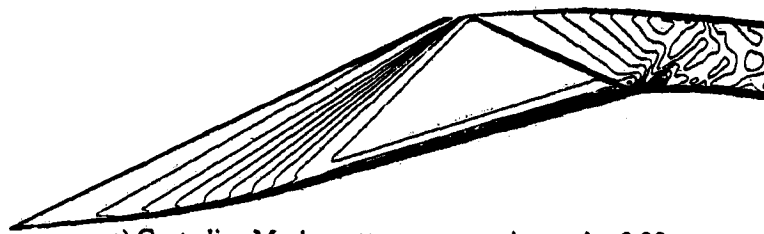


c) Ramp rake 1

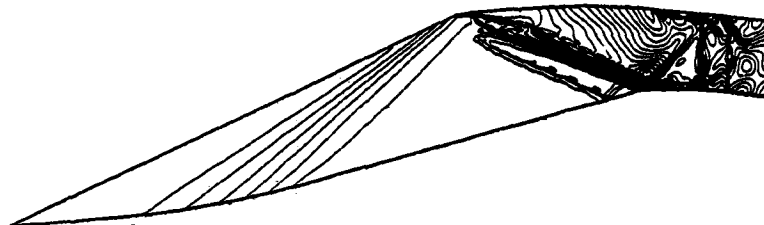


d) Ramp rake 2

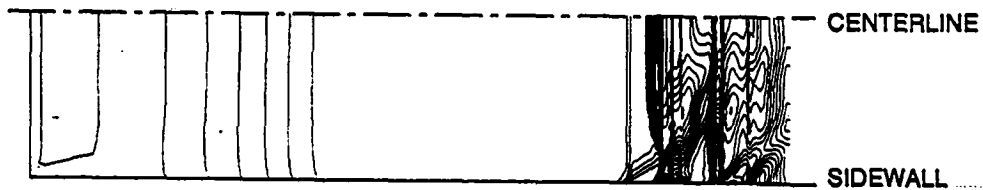
Fig. 6 NSS configuration results.



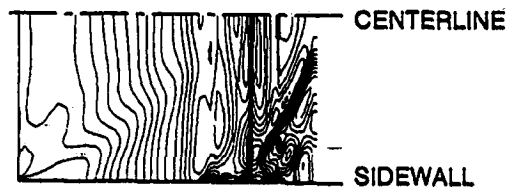
a) Centerline Mach contours, contour interval = 0.05



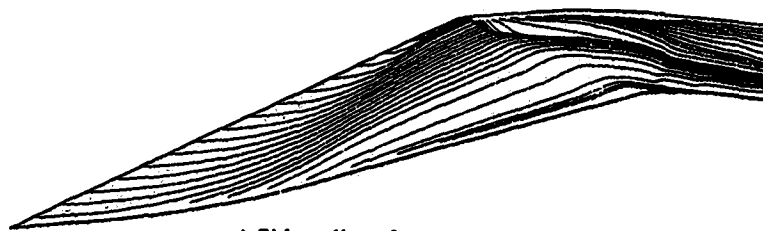
b) Sidewall pressure contours, contour interval = 0.2 P_o



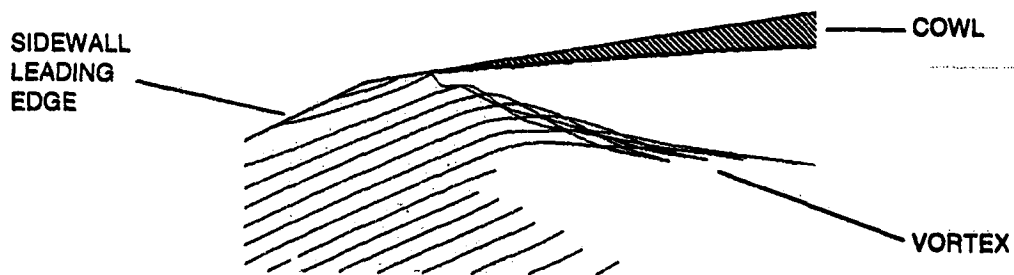
c) Ramp pressure contours, contour interval = 0.2 P_o



d) Cowl pressure contours, contour interval = 0.2 P_o



e) Sidewall surface streamlines



f) Sidewall detail: vortex due to cowl shock - sidewall boundary layer interaction

Fig. 7 Flow visualization of SS1 configuration results

REPORT DOCUMENTATION PAGE			Form Approved OMB No. 0704-0188	
Public reporting burden for this collection of information is estimated to average 1 hour per response, including the time for reviewing instructions, searching existing data sources, gathering and maintaining the data needed, and completing and reviewing the collection of information. Send comments regarding this burden estimate or any other aspect of this collection of information, including suggestions for reducing this burden, to Washington Headquarters Services, Directorate for Information Operations and Reports, 1215 Jefferson Davis Highway, Suite 1204, Arlington, VA 22202-4302, and to the Office of Management and Budget, Paperwork Reduction Project (0704-0188), Washington, DC 20503.				
1. AGENCY USE ONLY (Leave blank)	2. REPORT DATE December 1995	3. REPORT TYPE AND DATES COVERED Technical Memorandum		
4. TITLE AND SUBTITLE 3D Navier-Stokes Analysis of a Mach 2.68 Bifurcated Rectangular Mixed-Compression Inlet			5. FUNDING NUMBERS WU-537-02-22	
6. AUTHOR(S) M. Mizukami and J.D. Saunders				
7. PERFORMING ORGANIZATION NAME(S) AND ADDRESS(ES) National Aeronautics and Space Administration Lewis Research Center Cleveland, Ohio 44135-3191			8. PERFORMING ORGANIZATION REPORT NUMBER E-10038	
9. SPONSORING/MONITORING AGENCY NAME(S) AND ADDRESS(ES) National Aeronautics and Space Administration Washington, D.C. 20546-0001			10. SPONSORING/MONITORING AGENCY REPORT NUMBER NASA TM-107123 AIAA-96-0495	
11. SUPPLEMENTARY NOTES Prepared for the 34th Aerospace Sciences Meeting and Exhibit sponsored by the American Institute of Aeronautics and Astronautics, Reno, Nevada, January 15-18, 1996. Responsible person, M. Mizukami, organization code 2780, (216) 433-3387.				
12a. DISTRIBUTION/AVAILABILITY STATEMENT Unclassified - Unlimited Subject Category 07 This publication is available from the NASA Center for Aerospace Information, (301) 621-0390.			12b. DISTRIBUTION CODE	
13. ABSTRACT (Maximum 200 words) The supersonic diffuser of a Mach 2.68 bifurcated, rectangular, mixed-compression inlet was analyzed using a three-dimensional (3D) Navier-Stokes flow solver. A two-equation turbulence model, and a porous bleed model based on unchoked bleed hole discharge coefficients were used. Comparisons were made with experimental data, inviscid theory, and two-dimensional Navier-Stokes analyses. The main objective was to gain insight into the inlet fluid dynamics. Examination of the computational results along with the experimental data suggest that the cowl shock-sidewall boundary layer interaction near the landing edge caused a substantial separation in the wind tunnel inlet model. As a result, the inlet performance may have been compromised by increased spillage and higher bleed mass flow requirements. The internal flow contained substantial waves that were not in the original inviscid design. 3D effects were fairly minor for this inlet at on-design conditions. Navier-Stokes analysis appears to be an useful tool for gaining insight into the inlet fluid dynamics. It provides a higher fidelity simulation of the flowfield than the original inviscid design, by taking into account boundary layers, porous bleed, and their interactions with shock waves.				
14. SUBJECT TERMS Supersonic inlets; Computational fluid dynamics; Navier-Stokes equation			15. NUMBER OF PAGES 11	
			16. PRICE CODE A03	
17. SECURITY CLASSIFICATION OF REPORT Unclassified	18. SECURITY CLASSIFICATION OF THIS PAGE Unclassified	19. SECURITY CLASSIFICATION OF ABSTRACT Unclassified	20. LIMITATION OF ABSTRACT	